



**HAL**  
open science

# Nucleation and growth on a superhydrophobic grooved surface

R. Narhe, Daniel Beysens

► **To cite this version:**

R. Narhe, Daniel Beysens. Nucleation and growth on a superhydrophobic grooved surface. *Physical Review Letters*, 2004, 93 (7), 076103 (4 p.). 10.1103/PhysRevLett.93.076103 . hal-00160928

**HAL Id: hal-00160928**

**<https://hal.science/hal-00160928v1>**

Submitted on 9 Feb 2022

**HAL** is a multi-disciplinary open access archive for the deposit and dissemination of scientific research documents, whether they are published or not. The documents may come from teaching and research institutions in France or abroad, or from public or private research centers.

L'archive ouverte pluridisciplinaire **HAL**, est destinée au dépôt et à la diffusion de documents scientifiques de niveau recherche, publiés ou non, émanant des établissements d'enseignement et de recherche français ou étrangers, des laboratoires publics ou privés.

## Nucleation and Growth on a Superhydrophobic Grooved Surface

R. D. Narhe and D. A. Beysens\*

*Equipe CEA-CNRS du Supercritique pour l'Environnement, les Matériaux et l'Espace, Service des Basses Températures, CEA-Grenoble, Grenoble, France*

(Received 23 March 2004; published 13 August 2004)

The growth dynamics of water drops condensed on a superhydrophobic geometrically patterned surface were studied. Drop size evolution at early and intermediate times is self-similar. Drop growth laws do not differ for a flat surface because of a reduction of both drop and substrate dimensionality. A striking observation is the instantaneous drying of the top surface of grooves at a point in time due to coalescence of the drops with a completely filled channel. At late times, only a few large drops grow connected to the channels, in a mixed Wenzel-penetration regime.

DOI: 10.1103/PhysRevLett.93.076103

PACS numbers: 68.08.Bc, 47.85.Np, 64.60.Qb

Water drops on lotus leaves have attracted the interest of the scientific community [1–3]. The contact angle of such water drops is very large ( $>150^\circ$ ), and since this water cannot spread, it rolls about as small droplets, removing dirt. This phenomenon has important scientific and commercial applications. Recently, researchers have mimicked these superhydrophobic and self-cleaning properties of the lotus leaf [2], making possible active prevention of contamination (e.g., chemical and radioactive) of materials. However, it should be noted that water may come into contact on such a surface not only by projection or deposition, but also by condensation (nucleation and growth). This is a process that has not yet been considered and which can modify the interesting self-cleaning properties of a superhydrophobic surface. Accordingly, the present Letter reports on condensation in such a micropatterned surface. To our knowledge, there are no detailed reports of phase transition in geometrically patterned superhydrophobic surfaces, though we are aware of the research by Lafuma and Quéré [4] on (Wenzel) the drop situation where water fills the channel.

The general problem that we address here is thus twofold. Is superhydrophobicity preserved during condensation? What are the mechanisms of nucleation and growth in such microstructured patterns? The latter question also addresses general problems of droplet-based microfluidic systems, where phase transition is only rarely considered. We described below how, during the nucleation and growth process, unexpected and spectacular self-drying processes were discovered. Important reports regarding superhydrophobicity and self-cleaning properties are referred in [5–7]. In general, three wetting regimes were observed: air pocket regime [8], where air remains trapped below the drop (e.g., drop gently put on the substrate), Wenzel regime [9], where the above air pockets are filled with liquid (e.g., drop slightly pushed on the substrate), and penetration regime (e.g., drop firmly pushed on the substrate), where liquid fills also a region of the substrate around the drop.

Nucleation and growth of drops on a surface, whose dew or breath figures [10,11] are the most common representation of this phenomenon, is known to obey general self-similar growth laws [12]. The drop pattern grows as  $\langle R \rangle \sim t^{1/D_d}$  (early times, isolated drops) and  $\langle R \rangle \sim t^{1/(D_d-D_s)}$  (intermediate and late times, coalescing drops). Here  $R$  is the drop radius,  $t$  is time, and  $D_d$  and  $D_s$  are the drop and substrate dimensionality, respectively. In the present work, we investigate the effect that a grooved surface induces on such nucleation and growth processes. The substrate used was a piece of silicon wafer  $2 \times 1 \text{ cm}^2$ . Half of the wafer ( $1 \times 1 \text{ cm}^2$ ) was grooved to form a strip pattern structure of width “ $a$ ,” separation “ $b$ ,” height “ $c$ ,” and bottom diameter “ $d$ ” (see Fig. 1). The technique used for making such a grooved superhydrophobic surface is the same used by Yoshimitsu *et al.* [7]. Substrates with different combinations ( $a$ ,  $b$ ,  $c$ , and  $d$ ) are used in the present study (see Table I). They all exhibit the same behavior.

The details of substrate cleaning and the experimental procedure are given in [13]. The cleaned substrate is fixed on a thick electrolytic copper plate of the condensation chamber by thin liquid film in order to ensure good thermal contact. The gas flow (saturated with water vapor)

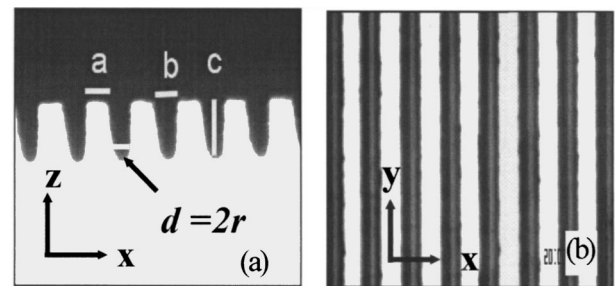


FIG. 1. Typical optical microscopic image of grooved patterned silicon substrate showing (a) the side view and (b) the top view.  $a = 22 \mu\text{m}$ ,  $b = 25 \mu\text{m}$ ,  $c = 52 \mu\text{m}$ , and  $d = 13 \mu\text{m}$ .

TABLE I. Grooved patterned silicon substrate used in the present study. The contact angle is  $\theta = 57^\circ$  without silanization and  $\theta = 90^\circ$  with silanization.

Sub. No.	Width $a$ ( $\mu\text{m}$ )	Separation $b$ ( $\mu\text{m}$ )	Height $c$ ( $\mu\text{m}$ )	Bottom diameter $d$ ( $\mu\text{m}$ )
1	22	25	52	13
2	34	55	82	16
3	43	28	102	10
4	66	58	89	26
5	113	89	102	40

rate was kept fixed at 0.6 L/min for all experiments. The thickness of the saturated air layer from the substrate to the upper part of the chamber is  $\approx 5$  mm. The temperature difference between the supersaturated water vapor and the substrate is  $8^\circ\text{C}$ . Observations verified that it was not possible to condense rainlike droplets in the saturated air. A simple calculation shows that homogeneous nucleation [14] should occur for an air temperature difference as large as  $25^\circ\text{C}$ . Hence, only heterogeneous nucleation is possible. Because pure  $\text{N}_2$  gas is passed through pure water, the only nucleation sites are on the substrate due to surface inhomogeneities. The growth of drops was observed with a charge coupled device (CCD) camera attached to an optical microscope (resolution  $\approx 5 \mu\text{m}$ ) and recorded on a video recorder. Video images were digitized and then analyzed.

The wetting properties of the substrate were changed by a silanization method (coated with decyltrichlorosilane) [15,16]. A sessile drop method [13] was used for measurement of the contact angle. The equilibrium value of the contact angle, defined as  $\theta = (\theta_a + \theta_r)/2$  was  $57 \pm 2^\circ$  for a patterned silicon substrate without coating ( $\theta_a = 64^\circ$  and  $\theta_r = 50^\circ$ ). For the silanized substrate, the contact angle was  $90 \pm 2^\circ$  on the unpatterned part of the substrate, and  $130 \pm 2^\circ$  ( $110 \pm 2^\circ$ ) in an orthogonal (parallel) direction of the groove on the patterned part of the substrate. The phenomena that we describe are similar for both studied contact angles ( $\theta = 57^\circ, 90^\circ$ ); however, some distinguishing features were found in the duration of the intermediate stages. We first describe and discuss the condensation process with  $\theta = 57^\circ$ . The following four stages of growth (Fig. 2) can be identified:

(1) *Initial and intermediate stages:  $2R < a, b \approx d$ .*—At the start of the gas flow, the nucleation of tiny water drops at the top surface as well as at the channel takes place. At this stage, where the surface coverage ( $\epsilon$ ) remains low [Fig. 3(a)], drops do not undergo coalescence and the average drop radius grows as for isolated drops. A fit to  $\langle R \rangle = \rho t^\alpha$  gives  $\alpha = 0.35 \pm 0.03$  and  $\rho = 14 \pm 0.45$  ( $R$  in  $\mu\text{m}$ ,  $t$  in min), in agreement with  $t^{1/D_d}$ , where  $D_d = 3$ . However, as the surface coverage increases, drop coalescence cannot be neglected any further. The coalescence process results in slightly non-

circular drops [Fig. 2 (stage 1)]. The growth law exponent becomes unity, in agreement with  $t^{1/(D_d - D_s)}$ , with  $D_d = 3$  and  $D_s = 2$  [Fig. 3(a)].

(2) *Intermediate stage:  $2R > a, b \approx d$ .*—The drop size now exceeds the channels and top width, and drops grow along the groove length where they are pinned, with an elongated shape. The directions  $x, y, z$  are defined in Fig. 1 and  $2R_x, 2R_y$  are the drop dimensions as defined in Fig. 2(b). At this stage one can observe a large number of elongated drops with  $2R_x = a, b$  that coalesce only in the  $y$  direction. This is because the capillary forces, which then to make the drop perimeter circular, are weaker than the pinning forces at the edge of the groove. Therefore, the drops can grow only in the  $y$  and  $z$  directions. A power law fit  $\langle R_y \rangle = \rho_y t^\beta$  gives  $\rho_y = 23 \pm 3.6$  ( $R$  in  $\mu\text{m}$ ,  $t$  in min) and  $\beta = 1.0 \pm 0.04$ , in agreement with  $t^{1/(D_d - D_s)}$ . The effective dimensionality of drops is indeed  $D_d = 2$  (growth only along  $y$  and  $z$  axes) and the substrate dimensionality is now  $D_s = 1$  (coalescence along the  $y$  axis). In the channel, where  $b < a$ , the drop anisotropy is much more pronounced, and the channels progressively fill in. At this stage, the surface coverage is high and

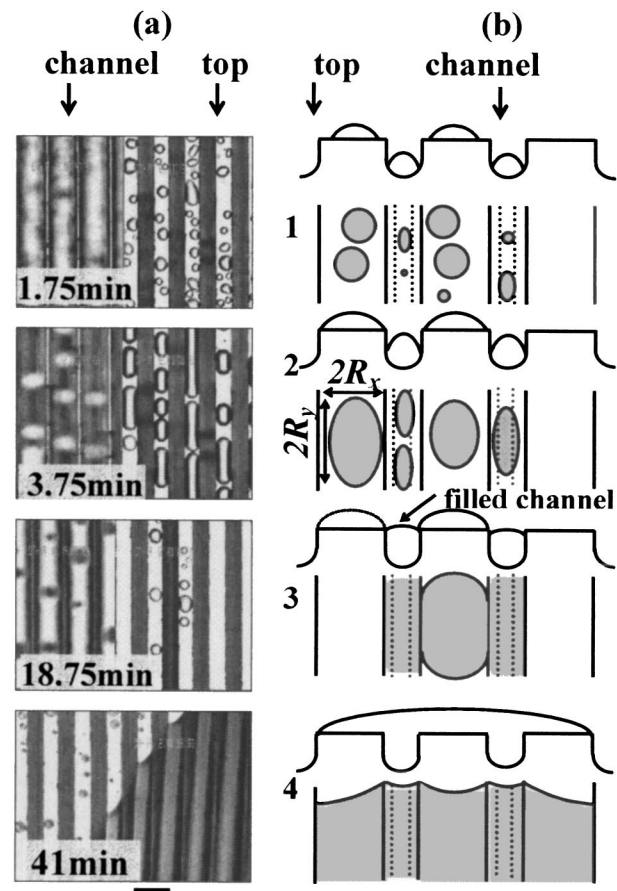


FIG. 2. Four growth stages of a condensed water drop with contact angle  $57^\circ$  on a patterned silicon substrate. (a) Microscopic picture and (b) schematic illustration. (Substrate No. 1. Bar is  $50 \mu\text{m}$ .)

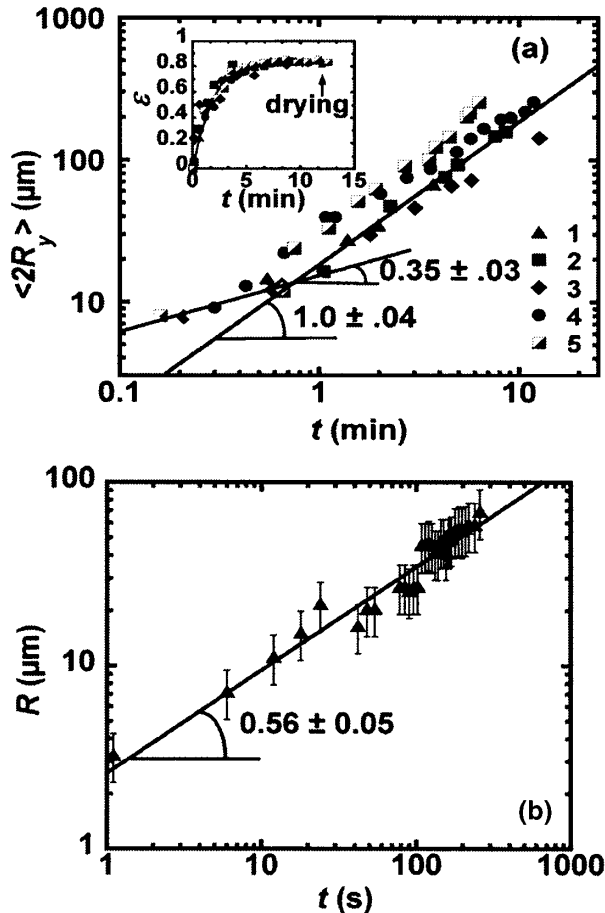


FIG. 3. Time evolution of (a)  $\langle 2R_y \rangle$ . The contact angle  $\theta$  is  $57^\circ$ . 1–5 refer to different substrate numbers (Table I). Inset: time evolution of surface coverage  $\epsilon$ . (b) Time evolution of radius  $R$  of a large drop formed at stage 4.

constant,  $\epsilon \approx 0.82$  [Fig. 3(a)], a signature of self-similar growth. Note that this value is in agreement with the empirical linear equation deduced from [17] on a flat 2D surface. Considering that the surface coverage is analogous to the random packing limit one deduces the 1D limit  $\epsilon_1$  from the 2D limit  $\epsilon_2$ , as  $\epsilon_1 = \sqrt{\epsilon_2}$ ; i.e.,  $\epsilon_1 = (1 - \theta/200)^{1/2}$ .

(3) *Drying stage*.—This is a quite interesting feature during growth. The water level in the channel reaches the top and coalesces with one drop at the top surface. This results in an increase of the water level in the channel and coalescence with additional drops. A chain reaction of coalescence follows, resulting in an instantaneous drying of one groove top surface adjacent to the channel. Occasionally the two adjacent top grooves were found to dry at the same time (Fig. 4). This drying process is very rapid ( $<20$  ms). In the drying process, all drops at the top instantaneously flow down into the channel, which is followed by new nucleation on this dried surface. This process develops progressively on the entire grooved surface with the drying time dependent on the exact channel geometry, which varies slightly over the sub-

strate. Gravity has no effect on the drops at the top surface during the drying stage since drops remain smaller than the capillary length of water ( $\approx 3$  mm). The drying is due only to the coalescence of drop(s) at the top and the channel. We have also confirmed the growth laws and growth stages by condensing the vapor from below onto the patterned substrate held upside down. The driving force is thus only from surface tension.

(4) *Large drop formation stage* ( $2R_x \gg a, b$ ).—Over time, the liquid level in the channel increases and bridges form between the channels. These bridges grow and eventually result in a few large drops covering many grooves. These drops grow mainly by collecting water from the channels connected to it. Assuming a constant condensation rate on the channels, one finds that the growth rate  $dR^3/dt \sim RL$ , with  $L$  the wafer length in the direction parallel to the grooves [Fig. 3(b)]. It should then follow a growth law  $R \sim t^{1/2}$ . Data from Fig. 3(b) can be indeed fitted to  $R = \rho_D t^\gamma$ , with  $\gamma = 0.56 \pm 0.05$  and  $\rho_D = 2.6 \pm 0.6$  ( $R$  in  $\mu\text{m}$ ,  $t$  in s).

In order to study drop growth dynamics, we measured  $2R_x$  and  $2R_y$ . However, we focused only on  $2R_y$  since it is the only measurable parameter for a long period of time. Figure 3(a) shows the time evolution of  $\langle 2R_y \rangle$ . At the initial stage, the drops are isolated and grow as  $\langle 2R_y \rangle \sim t^\alpha$ ,  $\alpha \approx 0.35$ . When coalescences dominate,  $\langle 2R_y \rangle \sim t^\alpha$ ,  $\alpha \approx 1$ . At this stage the drops are elongated and grow along the length of the groove. It is similar to a 2D drop growth on a 1D substrate. The inset is the time evolution of surface coverage ( $\epsilon$ ). At the initial stage, surface coverage increases rapidly due to drop growth. At the intermediate stage it levels off.

We also studied the growth dynamics of drops on a patterned silicon surface coated with decyltrichorosilane.

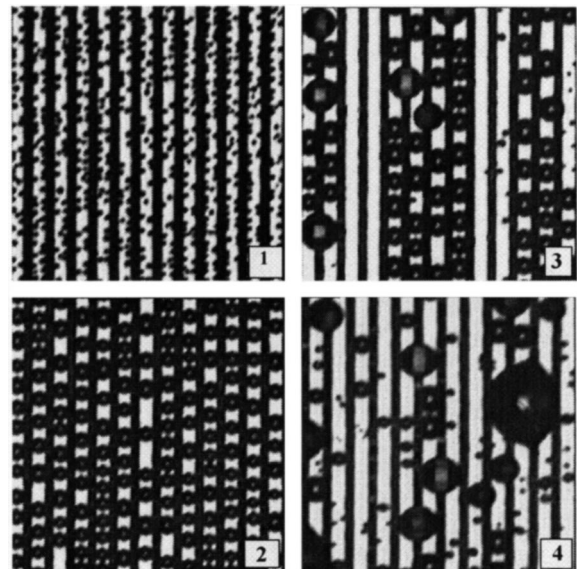


FIG. 4. The four growth stages of water drops on a grooved substrate for a contact angle of  $90^\circ$  ( $130^\circ$ ).

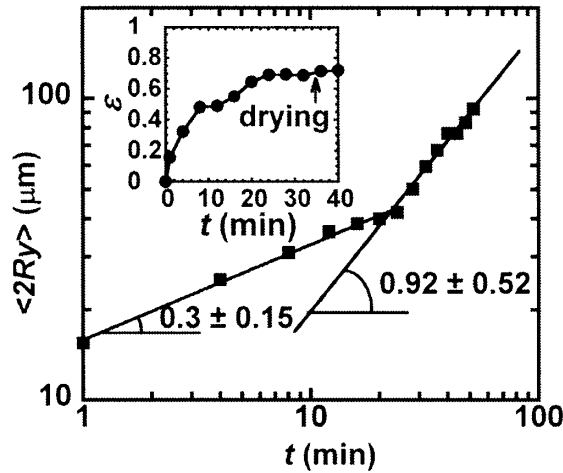


FIG. 5. Time evolution of  $\langle 2R_y \rangle$ . Inset: surface coverage  $\varepsilon$  vs time.  $\varepsilon$  remains constant at 0.71 in a self-similar regime; the value is in agreement for  $\theta = 90^\circ$  with  $\varepsilon_1 = (1 - \theta/200)^{1/2}$ .

The average defect size that we obtained from the relaxation of the composite drop method [13] is about  $10 \mu\text{m}$ . The contact angle  $\theta$  is  $90^\circ$  for  $2R_x < a$ , and  $130^\circ$ , for  $2R_x > a$ . For such coated surfaces, the nucleation rate and the  $R_x, R_y$  growth rate are markedly slower. We also observed and confirmed the four growth stages, especially the drying stage (Fig. 4) and the corresponding growth laws (Fig. 5), as discussed previously. Nevertheless, a few distinguishable features were noticed, such as (i) the absence of elongated drops during growth (Fig. 4), due to the importance of capillary forces with respect to the pinning forces and (ii) drops that sooner bridge the channels.

From the above, it is clear that air pocket superhydrophobicity does not occur during condensation on grooved substrates. In the last stage, condensation proceeds in a few large droplets fed by the grooves. These droplets are in the Wenzel regime perpendicular to the grooves and in the penetration regime parallel to them. Lafuma and Quéré [4] have already reported that condensation on a pillar microstructured surface led to the Wenzel drop. The fact that condensation in the last stage proceeds in a few large droplets fed by channels means that the wet surface

on the patterned substrate remains low when compared to the flat surface, which is a signature of superhydrophobicity. In addition, the groove top surface remains almost dry. In this sense, condensation on such substrates enables some of the interesting features of superhydrophobicity to be retained.

The authors are indebted to V. Nikolayev for useful comments and a critical reading of the manuscript.

\*Author to whom correspondence should be addressed at CEA-ESEME, ESPCI-PMMH, 10, rue Vauquelin, 75231, Paris, Cedex 5, France.

Electronic address: dbeyens@cea.fr

- [1] A. Otten and S. Herminghaus, *Langmuir* **20**, 2405 (2004).
- [2] R. Blossey, *Nat. Mater.* **2**, 301 (2003).
- [3] W. Brathlott and C. Neinhuis, *Planta* **202**, 1 (1997).
- [4] A. Lafuma and D. Quéré, *Nat. Mater.* **2**, 457 (2003).
- [5] T. Onda, S. Shibuichi, N. Satoh, and K. Tsujii, *Langmuir* **12**, 2125 (1996).
- [6] M. Miwa, A. Nakajima, A. Fujishima, K. Hashimoto, and T. Watanabe, *Langmuir* **16**, 5754 (2000).
- [7] Z. Yoshimitsu, A. Nakajima, T. Watanabe, and K. Hashimoto, *Langmuir* **18**, 5818 (2002).
- [8] A. Cassie and S. Baxter, *Trans. Faraday Soc.* **40**, 546 (1944).
- [9] R. Wenzel, *Ind. Eng. Chem.* **28**, 988 (1936).
- [10] D. Beysens and C. M. Knobler, *Phys. Rev. Lett.* **57**, 1433 (1986).
- [11] D. Beysens, A. Steyer, P. Guenoun, D. Fritter, and C. M. Knobler, *Phase Transitions* **31**, 219 (1991).
- [12] J. L. Viovy, D. Beysens, and C. M. Knobler, *Phys. Rev. A* **37**, 4965 (1988).
- [13] R. Narhe, D. Beysens, and V. S. Nikolayev, *Langmuir* **20**, 1213 (2004).
- [14] R. A. Sigsbee, in *Nucleation*, edited by A. C. Zettlemoyer (Marcel Dekker, New York, 1969).
- [15] M. K. Chaudhary and G. M. Whitesides, *Science* **256**, 1539 (1992).
- [16] H. Elwing, S. Welin, A. Askendal, U. Nilsson, and I. Lunström, *J. Colloid Interface Sci.* **119**, 203 (1987).
- [17] H. Zhao and D. Beysens, *Langmuir* **11**, 627 (1995).